



Photo-Electrochemical Water Splitting Behaviour of ZnO Phthalocyanine and TiO₂ Phthalocyanines

M.K. Anitha*, A. Sebastin Thangadurai†, A. Cyril‡

Abstract

This describes a study on the photo-electrochemical water splitting behaviour of phthalocyanines of ZnO and TiO₂ as photo electrocatalysts. Here is a breakdown of the key points of the findings in this study. Phthalocyanines of ZnO and TiO₂ were synthesized using hydrothermal synthesis. The crystallinity of ZnO and TiO₂ phthalocyanines was examined using X-ray diffraction (XRD) analysis. The results indicate that ZnO phthalocyanine has a high crystallinity with a wurtzite structure, and TiO₂ phthalocyanine has a high crystallinity with an Anatase structure. Field emission scanning electron microscopy (FESEM) was used to study the surface morphological features. The observations suggest that oxide nanoparticles are combined with organic phthalocyanine. UV-Vis spectroscopy was employed to analyse the light absorbance properties of the materials. ZnO phthalocyanine showed absorption peaks at 330 nm (corresponding to ZnO) and a broad peak between 530 and 730 nm. Similarly, TiO₂ phthalocyanine exhibited absorption peaks at 340 nm (corresponding to TiO₂) and a broad peak between 530 and 730 nm. The ZnO and TiO₂ phthalocyanines were prepared on FTO (Fluorine-doped

* Department of Industrial Chemistry, Alagappa University, Karaikudi-630003.

† PG & Research Department of Chemistry, St. Joseph's College, Tiruchirappalli, Tamil Nadu, India

‡ PG & Research Dept. of Chemistry, Raja Douraisingam Government Arts College, Sivagangai- 630 561, Tamil Nadu, India; cyrilchemistry@gmail.com (*Corresponding Author*)

tin oxide) substrates and used as photo electrocatalysts in photo-electrochemical water splitting experiments with a sacrificial electrolyte (1M Na₂S) under light illumination (100 mW/cm²). Linear Sweep Voltammetry (LSV) studies revealed that the ZnO phthalocyanine photoelectrode showed the current density of ~10.8 mA/cm² at 0.8 V (vs. Ag/AgCl) under light illumination and about ~8.8 mA/cm² in the dark. Similarly, the TiO₂ phthalocyanine photoelectrode showed the current density of ~10.5 mA/cm² at 0.8 V (vs. Ag/AgCl) under light illumination compared to ~7.8 mA/cm² in the dark. The Chronoamperometric (CA) studies observations indicated that the ZnO phthalocyanine photoelectrode had a higher current density of ~12.0 mA/cm² at 0.8 V (vs. Ag/AgCl) under light illumination compared to ~9.0 mA/cm² in the dark. The TiO₂ phthalocyanine photoelectrode demonstrated a similar trend with a higher current density under light compared to the dark. This study's key finding is that the ZnO phthalocyanine has demonstrated a higher current density than that of TiO₂ phthalocyanine in both LSV and CA measurements under light illumination. In summary, this work demonstrates the enhanced photo-electrochemical water splitting activity of ZnO phthalocyanine compared to TiO₂ phthalocyanine. This finding has implications for improving the efficiency of photo electrocatalysts for water splitting applications and contributes to understanding these materials' performance in renewable energy generation.

Keywords: Photo-Electrochemical Water Splitting, ZnO Phthalocyanine, TiO₂ Phthalocyanines

Introduction

The development of stable catalysts for semiconductor-based photocatalysis is becoming increasingly important in the field of materials science research and development. This is because the production of clean hydrogen fuel through water splitting has significant potential for addressing energy and environmental challenges [1-2]. The work of Fujishima and Honda in 1972, who

reported the photo-electrochemical water splitting using TiO_2 semiconductor became a landmark discovery and marked the beginning of extensive research efforts in the field of photocatalysis for water splitting [3]. Visible light absorption is crucial for efficient solar water splitting because the solar spectrum contains nearly 50% visible light in the wavelength range of 400 to 800 nm. To harness solar energy effectively, photocatalysts should be capable of absorbing this visible light. Researchers have commonly investigated semiconductor-based metal oxides like TiO_2 , WO_3 , ZnO , and SnO_2 for use as photocatalysts in solar water electrolysis. These metal oxides, while useful, have limitations [4-7]. They typically exhibit inadequate absorption of visible light, which is a significant portion of the solar spectrum. Additionally, they may lack a negative conduction band (CB), which is essential for facilitating the hydrogen evolution reaction (H_2 generation). One crucial requirement for efficient light-harvesting systems is that the sensitizer molecule should possess directionality. This directional behaviour can be achieved by incorporating “push” (electron-donating) and “pull” (electron-withdrawing) functional groups as substituents on the phthalocyanine (Pc) ring. These functional groups influence the movement of electrons within the molecule [8]. Phthalocyanines have been employed as photocatalysts in the presence of ZnO or TiO_2 materials. These materials are known for their photocatalytic properties and are commonly used in various applications, including water splitting, pollutant degradation, and solar energy conversion [9-11]. One promising candidate is the conjugated molecule of Copper (II) phthalocyanine covalent organic framework (CuPc-COF) dye material. CuPc has been shown to form a variety of polymorphisms, reported as monoclinic, tetragonal, orthorhombic, and triclinic [12]. The CuPc-COF is a strong light absorbing organic material. In CuPc, containing 20% of nitrogen and 10% of copper having a paramagnetic character with one unpaired electron and lead have a high chemical and thermal resistance. The CuPc has potential applications in gas sensors, organic field effect transistors (OFETs), optical storage, optical switches, and organic photovoltaic cells (OPVCs) [13-20]. Indeed, CuPc has been used in many areas of quantum computing, pigments, and paper industry. The CuPc used as an electrocatalyst for hydrogen gas preparation previously reported [21-22]. Zhang et al. reported that the

photocatalytic properties of CuPc on Electro spun TiO₂ Nanofibers [23]. It is also reported that the photoelectrical conversion efficiency of the TiO₂ solar cells, was greatly improved with the sensitization of CdSe [24-25] and tetra carboxyl zinc phthalocyanine. Much research has been done on CuPc, however, the combinational approach in connection with ZnO or TiO₂ phthalocyanine would certainly be beneficial in photoelectrochemical water splitting activity, where such kind of attempts have not been reported. Hence, this work focuses on the study of the photoelectrochemical water splitting behaviour of ZnO and TiO₂ phthalocyanines. It is noticed that the enhanced photoelectrochemical water splitting activity for ZnO phthalocyanine compared to TiO₂ phthalocyanine. This finding has implications for improving the efficiency of photo electrocatalysts for water splitting applications and contributes to the understanding of these materials' performance in renewable energy generation.

Experimental Procedure

Synthesis of ZnO:

In the preparation of a ZnO solution through hydrothermal synthesis, 0.5 M solution of zinc nitrate (Zn (NO₃)₂) is prepared by dissolving the appropriate amount of zinc nitrate in 30 ml of distilled water. Stirring is employed for 30 minutes to ensure the complete dissolution of zinc nitrate in water. Simultaneously, a 5 M solution of sodium hydroxide (NaOH) is prepared by dissolving weighed pellets of sodium hydroxide in 30 ml of distilled water. Similar to the previous step, stirring is performed for 30 minutes to achieve a homogeneous NaOH solution. The sodium hydroxide (NaOH) solution is added dropwise to the zinc nitrate (Zn (NO₃)₂) solution while continuously stirring. The goal is to adjust the pH of the reactants to a value of 12. This adjustment is crucial for controlling the reaction conditions and promoting the formation of ZnO. The resulting solution mixture, with a pH of 12, is transferred into Teflon-lined sealed stainless-steel autoclaves. Autoclaves are used to create a sealed, high-pressure environment that is ideal for hydrothermal reactions. The sealed autoclaves containing the solution mixture are placed in a hydrothermal oven and maintained at a temperature of 120 °C for a duration of 2 h. This hydrothermal reaction is essential for the

synthesis of ZnO nanoparticles or crystals. After the hydrothermal reaction is completed, the autoclaves are removed from the oven. The solution inside the autoclaves is allowed to cool naturally to room temperature. This cooling step is important to stabilize the synthesized ZnO and prevent rapid temperature changes [12-15].

Synthesis of TiO₂:

The starting material is pure TiO₂ powder (Degussa P25) with a particle size of 25 nm. This TiO₂ powder has a crystalline structure that is a mixture of anatase and rutile phases in an 80:20 ratio. 0.5 grams of the TiO₂ powder are added to an aqueous solution of sodium hydroxide (NaOH) with a concentration of 10 M and a volume of 40 ml. The mixture is vigorously stirred for 30 minutes. This step likely helps in the dispersion of the TiO₂ particles in the NaOH solution. The TiO₂-NaOH mixture is then transferred to a 50 mL Teflon-lined stainless-steel autoclave. The autoclave is sealed to create a high-pressure, high-temperature environment. The hydrothermal treatment takes place at a temperature of 200°C for a duration of 48 h. This extended treatment period is typical for the hydrothermal synthesis of TiO₂ nanostructures and allows for controlled growth and crystallization. After the hydrothermal reaction, a white precipitate form. This precipitate likely consists of the synthesized TiO₂ nanostructures. The white precipitate is separated from the autoclave and allowed to cool naturally to room temperature. After cooling, the precipitate is washed with a 0.1 M hydrochloric acid (HCl) solution to remove any impurities or excess reactants. Subsequently, it is washed with deionized water to further purify the TiO₂ nanostructures [26-31].

Preparation of ZnO PC and TiO₂ PC:

Complexation of PC onto the surface of ZnO and TiO₂ nanoparticles is described below: The PC is dissolved in a solvent mixture of acetonitrile and ethanol in a 1:1 ratio to create a solution with a concentration of 75 mM. This solution is prepared in two separate reaction vessels. The ZnO and TiO₂ nanoparticles, which have been calcined (processed at high temperatures to remove impurities), are each immersed separately in the individual PC solutions. The immersion takes place overnight in sealed containers, and the containers are kept in the dark during this period. After the overnight

immersion, the nanoparticles are retrieved from their respective PC solutions. The retrieved functionalized nanoparticles, which appear blue, are washed with ethanol and dried in vacuum is a common technique to remove any remaining solvent and ensure that the functionalized nanofibers are dry and ready for further use.

Photo Electrochemical Water Splitting Studies:

The process conditions for conducting photo-electrochemical water splitting experiments using a three-electrode configuration is mentioned here. The working electrode is made of a conductive material coated with the photocatalyst material. In this case, it is coated with the material of interest (ZnO and TiO₂, phthalocyanines) and is referred to as the photoanode. Platinum foil serves as the counter electrode, and Ag/AgCl is used as the reference electrode. A sacrificial electrolyte consisting of 1M Na₂S with a pH of 13 is used. This electrolyte plays a crucial role in the water-splitting process and is sacrificial because it is consumed during the reaction. A 300 W Xenon lamp is used for illumination. The light intensity on the surface of the photoanode is maintained at 100 mW/cm². The light source is an essential component for initiating the photocatalytic reactions. Linear sweep voltammograms (LSV) are recorded by varying the potential between -0.8 V and 0.8 V relative to the Ag/AgCl reference electrode. The scan rate is set at 5 mV/s. LSV is a technique used to study the electrochemical behaviour of the photoanode under illumination. The stability of the photo-electrocatalyst is assessed using the chronoamperometry technique for extended periods. The electrolytic solution is bubbled through nitrogen gas. This is done to remove dissolved oxygen from the solution, as the presence of oxygen can interfere with the photocatalytic reactions.

Characterizations:

The absorption spectrum of the samples in the UV-VIS region (200-1200 nm) was recorded on a (Varian Cary 5000) UV-Vis NIR spectrophotometer. FT-IR (Fourier Transform Infrared spectroscopy) was obtained transmittance data on FT-IR spectrometer (Bruker Tensor 27). X-ray diffraction pattern was recorded on an (XRD Bruker D8-Advanced, Germany) angle between 10 °- 90 ° angle with 6 ° per min. Electrochemical workstation PARSTAT 2273 with power suite.

Results and Discussion

X-ray Diffraction Analysis:

The phase purity and crystallinity of ZnO and TiO₂ phthalocyanines are examined using X-Ray diffraction (Bruker-Advanced D8,) analysis and presented in Figure 1 and Figure 2, respectively. Figure 1 shows the peaks for wurtzite phase ZnO along with the additional peaks corresponding to PC. Similarly, Figure 2 shows the peaks for anatase phase TiO₂ along with the additional peaks corresponding to PC [32-37] and standard JCPDS file 98-000-5227. The Debye Scherrer equation, $D = K\lambda / \beta \cos\theta$, is used to calculate the crystalline size of the nanoparticles, where D is the nanoparticles crystalline size, K represents the Scherrer constant (0.98), λ denotes the wavelength (1.54), β denotes the full width at half maximum (FWHM). It is calculated that 90 nm for ZnO Pc and 85 nm for TiO₂ PC.

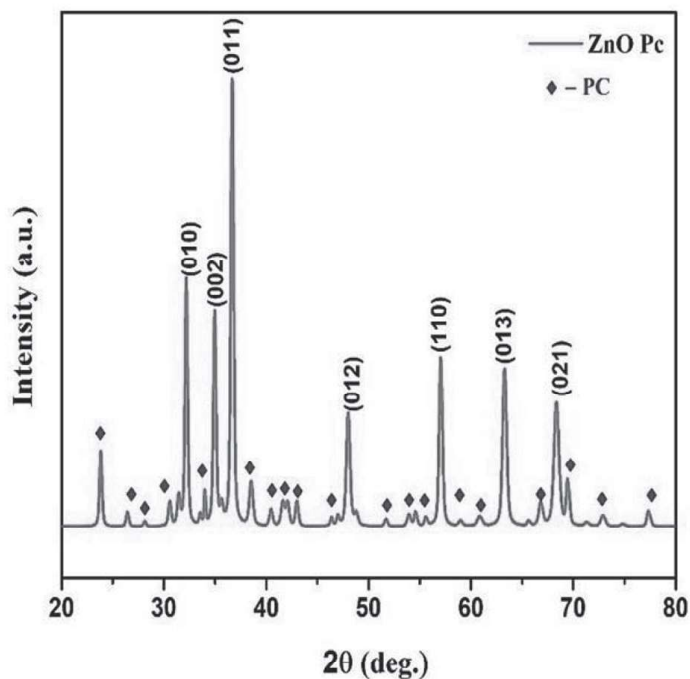
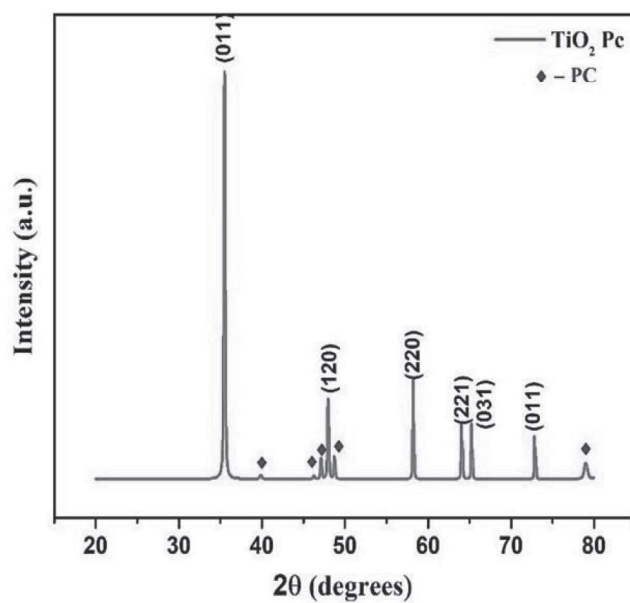


Figure 1: X-Ray diffraction pattern for ZnO PC

Figure 2: X-Ray diffraction pattern for TiO₂ PC

UV-Vis Spectra:

The UV-visible spectra were recorded using (Speccord 200 Plus, 200-800 nm). The UV-visible spectra of ZnO and TiO₂ phthalocyanines are shown in Figure 3 and Figure 4, respectively.

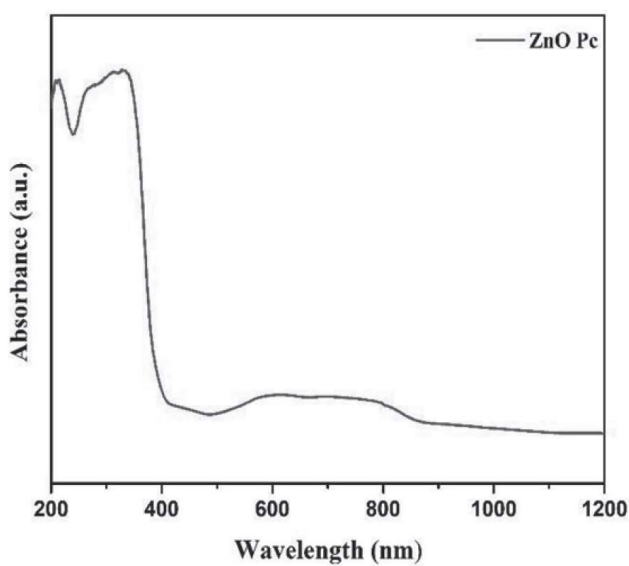


Figure 3: UV-vis absorbance spectra of ZnO PC

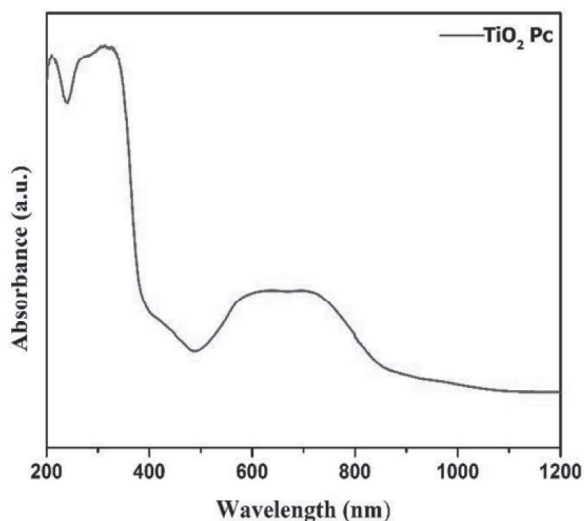


Figure 4: UV-vis absorbance spectra of TiO₂ PC

The ZnO phthalocyanine showed absorption peaks at 330 nm (corresponding to ZnO) and a broad peak between 530 and 730 nm. The band gap of ZnO Pc is calculated as 1.55 eV. Similarly, TiO₂ phthalocyanine exhibited absorption peaks at 340 nm (corresponding to TiO₂) and a broad peak between 530 and 730 nm [32-37]. The band gap of TiO₂ Pc is calculated as 1.78 eV.

Fourier-Transform Infrared (FT-IR) Spectroscopy:

FT-IR spectroscopy was used to understand the functional groups, which are present in ZnO PC and TiO₂ PC and the respective spectrums are shown in Figure 5 and 6, respectively.

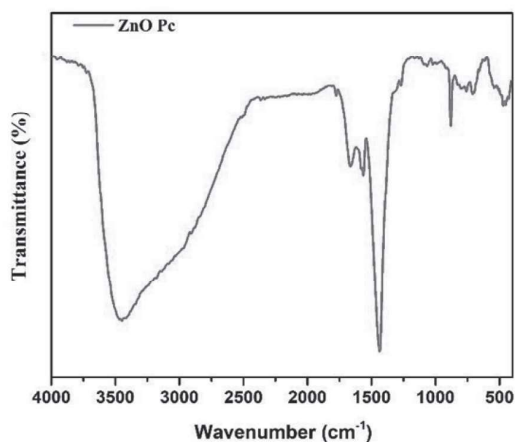


Figure 5: FTIR spectrum of ZnO PC

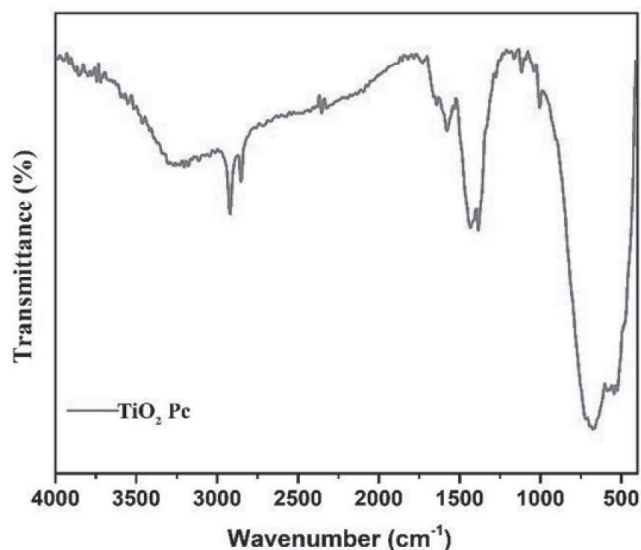


Figure 6: FTIR spectrum of TiO₂ PC

Figure 4, the spectrum shows peak at $\sim 460 \text{ cm}^{-1}$ corresponding to the vibration of hexagonal ZnO [32-37]. The spectrum shows peaks at 1330 cm^{-1} (C-N stretch), 1735 cm^{-1} (C=O stretch) and 3300 cm^{-1} (O-H stretch) attributed to the presence of the Pc. Similarly, Figure 5, spectrum shows peaks at 480 cm^{-1} and 732 cm^{-1} which are attributed to the O-Ti-O bonding in anatase. The peak at 3100 cm^{-1} attributed to the adsorbed hydroxyl groups [38-43].

Raman Spectroscopy:

Raman spectroscopy was used to understand the vibrational bands, which are present in ZnO PC and TiO₂ PC and the respective spectrums are shown in Figures 7 and 8, respectively. The D (at 1000 cm^{-1}) and G (1500 cm^{-1}) characteristic carbon material bands [27,28]

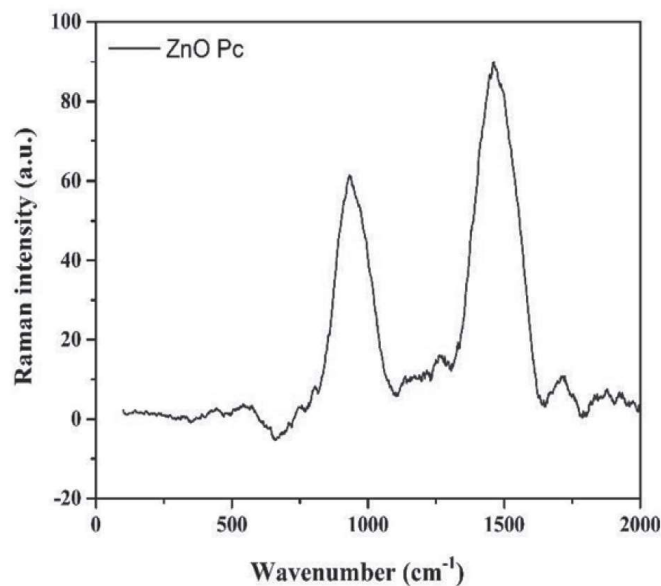


Figure 7: Raman spectrum of ZnO PC

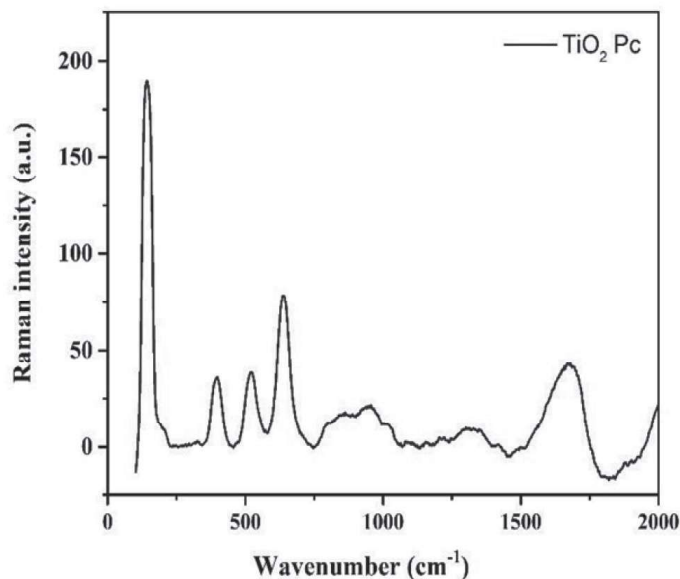


Figure 8: Raman spectrum of TiO₂ PC

Surface Morphological Analysis:

The surface morphologies of ZnO PC and TiO₂ PC are shown Figure 9 and Figure 10, respectively. The FESEM images of ZnO PC show the irregular shaped nanoparticles for and a similar observation noticed for TiO₂ PC also.

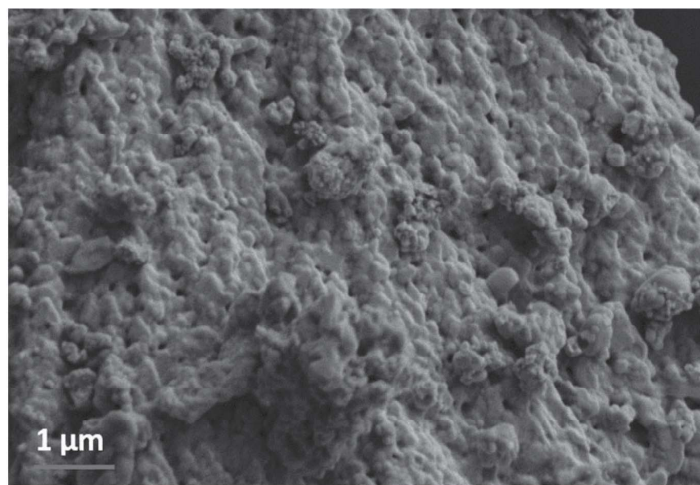


Figure 9: FESEM images of ZnO PC

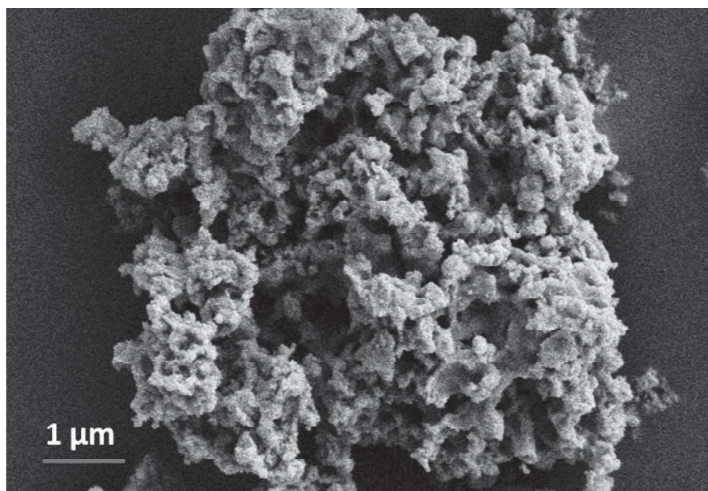


Figure 10: FESEM images of TiO₂ PC

Photo-Electrochemical Water Splitting:

Photoelectrochemical water splitting activities were analysed in three electrode systems using Auto lab potentiostat. The effective electrochemical area of the anode was maintained at 1 cm² and illuminated with a solar-simulator (100 mW/cm² using 300 W Xe lamp having AM 1.5G filter). The photoelectrochemical anodes of ZnO PC and TiO₂ PC were used as working electrodes in an aqueous solution of 1 M Na₂S sacrificial electrolyte.

The LSV curves of ZnO PC indicating the photoelectrochemical water splitting its activity under light and dark conditions is shown in Figure 11.

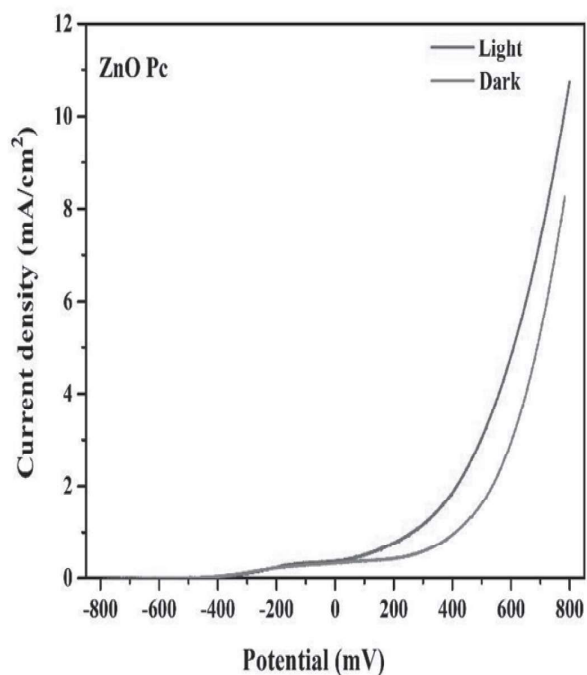


Figure 11: LSV curves of ZnO PC under dark and illumination conditions

The LSV curves indicate that the photoanode ZnO PC demonstrated higher current densities under light than those of dark. Linear Sweep Voltammetry (LSV) studies revealed that the ZnO phthalocyanine photoelectrode showed the current density of ~ 10.8 mA/cm² at 0.8 V (vs. Ag/AgCl) under light illumination and about ~ 8.5 mA/cm² in the dark. The Chronoamperometric (CA) studies observations (Figure 12) indicated that the ZnO phthalocyanine photoelectrode had a higher current density of ~ 12.0 mA/cm² at 0.8 V (vs. Ag/AgCl) under light illumination compared to ~ 9.0 mA/cm² in the dark.

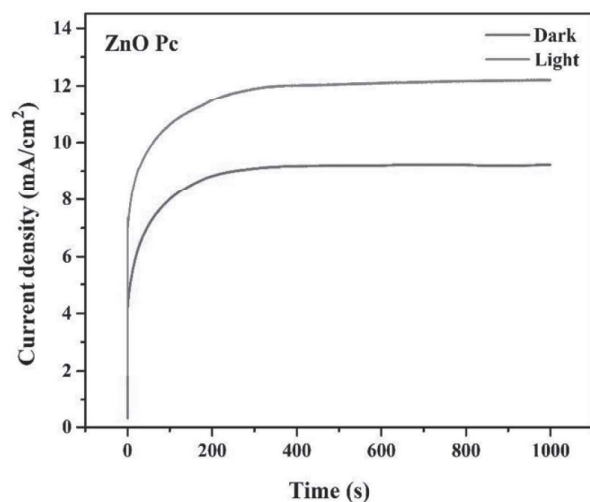


Figure 12: Chronoamperometric analysis of ZnO PC under dark and illumination conditions

The LSV curves of TiO_2 PC indicating the photoelectrochemical water splitting its activity under light and dark conditions is shown in Figure 13.

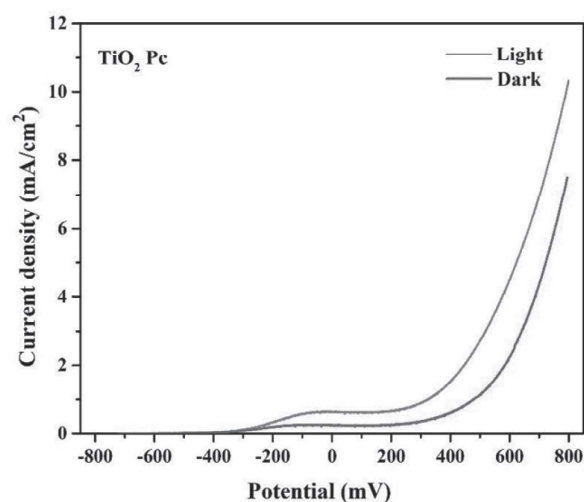


Figure 13: LSV curves of TiO_2 PC under dark and illumination conditions

The TiO_2 phthalocyanine photoelectrode showed the current density of $\sim 10.5 \text{ mA/cm}^2$ at 0.8 V (vs. Ag/AgCl) under light illumination compared to $\sim 7.8 \text{ mA/cm}^2$ in the dark. The Chronoamperometric (CA) studies observations indicated that the TiO_2 phthalocyanine photoelectrode had a higher current density of $\sim 10.8 \text{ mA/cm}^2$ at 0.8 V (vs. Ag/AgCl) under light illumination compared to $\sim 7.8 \text{ mA/cm}^2$ in the dark. The TiO_2 phthalocyanine photoelectrode demonstrated a

similar trend with a higher current density under light compared to in the dark.

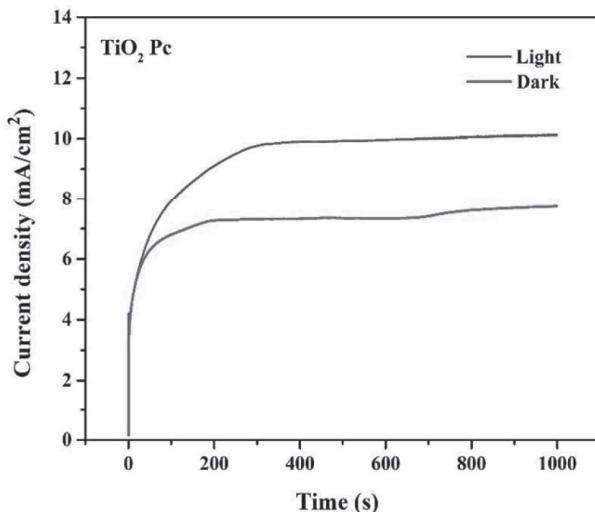


Figure 14: Chronoamperometric analysis of TiO₂ PC under dark and illumination conditions

This study reveals that the ZnO phthalocyanine demonstrated a higher current density than TiO₂ phthalocyanine in both LSV and CA measurements under light illumination. One dimensional morphology also improves the charge-carrying capacity and subsequently enhances the PEC efficiency. Also, the surface roughness would lead to micro pores, which increase the surface area and enhance the water splitting activity. The ZnO PC enhanced behaviour attributed to the smaller band gap (1.5 eV) in comparison with TiO₂ PC (1.78 eV).

Conclusion

The ZnO PC and TiO₂ PC have been synthesized successfully and explored as photo electrocatalyst in 1 M Na₂S electrolytes. The linear sweep voltammetry (LSV) studies revealed that the ZnO phthalocyanine photoelectrode showed the current density of ~10.8 mA/cm² at 0.8 V (vs. Ag/AgCl) under light illumination and about ~8.8 mA/cm² in the dark. The TiO₂ phthalocyanine photoelectrode showed the current density of ~10.5 mA/cm² at 0.8 V (vs. Ag/AgCl) under light illumination compared to ~7.8 mA/cm² in the dark. This study reveals that the ZnO phthalocyanine demonstrated a higher current density than that of TiO₂ phthalocyanine in both LSV and CA measurements under light illumination.

References

- [1] M. G. Walter, E. L. Warren, J. R. McKone, S. W. Boettcher, Q. Mi, E. A. Santori and N. S. Lewis, *Chem. Rev.*, 110, 6446 (2010).
- [2] X. Li, J. Yu, J. Low, Y. Fang, J. Xiao and X. Chen, *J. Mater. Chem. A*, 3, 2485 (2015).
- [3] A. Fujishima and K. Honda, *Nature*, 238, 37 (1972).
- [4] R. Saito, Y. Miseki and K. Sayama, *Chem. Commun.*, 48, 3833 (2012).
- [5] S. Hernández, D. Hidalgo, A. Sacco, A. Chiodoni, A. Lamberti, V. Cauda, E. Tresso and G. Saracco, *Phys. Chem. Chem. Phys.*, 17, 7775 (2015).
- [6] J. Su, L. Guo, N. Bao and C. A. Grimes, *Nano Lett.*, 11, 1928 (2011).
- [7] F. E. Osterloh, *Chem. Soc. Rev.*, 42, 2294 (2013).
- [8] L. Giribabu, C. V. Kumar, V. G. Reddy, P. Y. Reddy, C. S. Rao, S.-R. Jang, J.-H. Hum, M. K. Nazeeruddin and M. Graetzel, *Sol. Energy Mater. Sol. Cells*, 2007, 91, 1611-1616.
- [9] X. Wang, J. Gao, B. Xu, T. Hua and H. Xia, *RSC Adv.*, 2015, 5, 87233-87240.
- [10] H. You and Y. Zhao, *J. Phys. Chem. Biophys.*, 2016, 6, 1000199.
- [11] P. Khoza and T. Nyokong, *J. Coord. Chem.*, 2015, 68, 1117-1131.
- [12] Raji R and Gopchandran K G 2017 ZnO nanostructures with tunable visible luminescence; effects of kinetics of chemical reduction and annealing 2 51-8
- [13] Selim H, Nada A A, El-Sayed M, Hegazey R M, Eglal R S and Kotkata M F *Nano Science and Nano Technology: An Indian Journal*, 2018, 12, 122
- [14] Shanavas Khan J, Radhakrishnan A and Beena B *Indian Journal of Advances in Chemical Science*, 2018, 6, 2320-0898
- [15] Quadri T W, Lukman O, Fayemi O E, Solomon M M and Ebenso E E, *ACS Omega*, 2017, 2, 8421-37
- [16] Saeid Zanganeh, Amir Kajbafvala, Navid Zanganeh, Roya Molaei, M.R. Bayati, H. R. Zargar, S.K. Sadrnezhaad, *Adv. Powder Technol* 22 (2011) 336-339.
- [17] M. Qamar, C.R. Yoon, H.J. Oh, N.H. Lee, K. Park, D.H. Kim, K.S. Lee, W.J. Lee, S.J. Kim, *Catal. Today* 131 (2008) 3-14.

- [18] A.J. Maira, J.M. Coronado, V. Augugliaro, K.L. Yeung, J.C. Conesa, J. Soria, *J. Catal.* 2 (2001) 413–420.
- [19] C.T. Nam, W.D. Yang, L.M. Duc, et al., *Bull. Mater. Sci.* 36 (2013) 779–788.
- [20] L. Cui, K.N. Hui, K.S. Hui, S.K. Lee, W. Zhou, Z.P. Wan, Chi-Nhan Ha Thuc, *Mater. Lett.* 75 (2012) 175–178.
- [21] Srimala Sreekantan, Lai Chin Wei, *J. Alloys Compd.* 490 (2010) 436–442.
- [22] Mapukata, S., & Nyokong, T. (2020). Development of phthalocyanine functionalised TiO₂ and ZnO nanofibers for photodegradation of Methyl Orange. *New Journal of Chemistry*. doi:10.1039/d0nj03326j
- [23] L. Alagna, A. Capobianchi, M. P. Casaletto, G. Mattogno, A. M. Paoletti, G. Pennesi and G. Rossi, *J. Mater. Chem.*, 2001, 11, 1928–1935.
- [24] F. Chindeka, P. Mashazi, J. Britton, D. O. Oluwole, S. Mapukata and T. Nyokong, *J. Photochem. Photobiol., A*, 2020, 399, 112612.
- [25] B. D. Viezbicke, S. Patel, B. E. Davis and D. P. Birnie, *Phys. Status Solidi B*, 2015, 252, 1700–1710.
- [26] Z. Huang, B. Zheng, S. Zhu, Y. Yao, Y. Ye, W. Lu and W. Chen, *Mater. Sci. Semicond. Process.*, 2014, 25, 148–152.
- [27] C. Dette, M. A. Pe´rez-Osorio, C. S. Kley, P. Punke, C. E. Patrick, P. Jacobson, F. Giustino, S. J. Jung and K. Kern, *Nano Lett.*, 2014, 14, 6533–6538.
- [28] S. Bagheri, K. Shameli and S. B. A. Hamid, *J. Chem.*, 2013, 1–5.
- [29] G. Soler-Illia, A. Louis and C. Sanchez, *Chem. Mater.*, 2002, 14, 750–759